Journal of Applied Polymer Science

# Creatinine adsorption capacity of electrospun polyacrylonitrile (PAN)-zeolite nanofiber membranes for potential artificial kidney applications

**Limin Lu, Champika Samarasekera, John T.W. Yeow**
Department of Systems Design Engineering, University of Waterloo, Waterloo Ont., Canada
Correspondence to: J.T.W. Yeow (E-mail: jyeow@uwaterloo.ca)

**ABSTRACT:** Innovative dialysis membranes are needed for dialysis, which is the primary treatment for patients with end stage renal disease. In this study, we developed a polyacrylonitrile zeolite nanofiber composite membrane using an electrospinning process to adsorb uremic toxins through molecular sieve mechanism. Scanning electron microscope images revealed that the average diameter of the fiber fabricated with 10 wt % polyacrylonitrile was 673 nm and that of polyacrilonitirle-zeolite membranes were 277−419 nm. The creatinine adsorption behavior of 500-KOA (L), 720-KOA (Farrierite), 840-NHA (ZSM-5), and 940-HOA (Beta) zeolite powders were investigated. Among all the zeolites, 940-HOA zeolites showed the best performance. The creatinine adsorption capacity of 940-zeolite powders increased from 2234 μg/g in 50 μmol/L creatinine solution to 25423 μg/g in 625 μmol/L creatinine solution. The speed of adsorption was very quick; 0.025 g of 940-zeolite powders can eliminate 91% of 2 μmol creatinine in 5 min. The zeolites incorporated inside the membrane had higher creatinine adsorption capacity than free zeolites. © 2015 Wiley Periodicals, Inc. J. Appl. Polym. Sci. **2015**, *132*, 42418.

**KEYWORDS:** adsorption; composites; electrospinning

Received 16 February 2015; accepted 30 April 2015
**DOI: 10.1002/app.42418**

## INTRODUCTION

The kidney is an essential organ to the health of human beings. Its main function is to remove metabolic waste products, to regulate and eliminate extra cellular fluids and to help maintain hemostasis of the body. Kidney or renal failure is the complete or partial loss of the normal kidney function. This is characterized by its inability to remove excess water and metabolic wastes from the body. When kidney failure occurs, medical treatments are needed to keep the patients alive. Dialysis and kidney transplantation are two available treatments. Usually, dialysis is performed as the "bridge" to kidney transplantation since it sustains the life and health of patients as they wait for a donated kidney. In hemodialysis, a patient's blood is pumped to the blood compartment of a dialyzer, which is constituted by a bundle of semi-permeable hollow fiber membranes. When the blood flows inside the hollow fiber and dialysate flows in the space surrounding the hollow fiber, the excess wastes from the blood travel through the semi-permeable membrane to the dialysate. More than 70% of 615,000 end stage renal disease patients are on dialysis in America.[1] Although several types of hollow fiber dialysis membranes which eliminating uremic toxins though diffusion process are used in clinics,[2–5] the dialysis process is still inconvenient, time consuming, and expensive.

Patients with kidney failure have uremic toxins buildup, which are toxic to the body at high concentration and lead to a complex mixture of organ dysfunctions if left untreated.[6] Urea and creatinine are the common uremic toxins accumulated in chronic renal failure patients. The average concentration of urea and creatinine in patients are 38,333 ± 18,333 and 1204 ± 407 μmol, while that of normal health persons are less than 6700 and 106 μmol, respectively.[7] Uremic toxins can also be eliminated by adsorption other than the traditional diffusion mechanism which are used in dialyzers nowadays. In previous research,[8–11] zeolites powders are used to adsorb uremic toxins. Zeolites are the most commonly used crystalline materials for molecular sieves since various types of them can be easily obtained either from nature or synthesized in lab. The molecular sieve properties of zeolites as well as the fact that zeolites are nontoxic and very stable under physiological conditions make them a considered alternative method to eliminate uremic toxins in artificial kidney application. By analyzing the structure of a given zeolite, especially its pore size information, one can estimate what molecules the zeolite can adsorb.

In order to use zeolites to adsorb uremic toxins, zeolites can be incorporated into a nonporous polymer to form a composite membrane which has both the properties of molecular sieving

Additional Supporting Information may be found in the online version of this article.

and processability.[12] Polymer membranes with zeolite fillers were investigated in depth for water purification[13,14] and gas separation.[15,16] Nonwoven nanofibrous membranes, which can be produced through a simple electrospinning method, are an excellent choice for incorporating zeolite powders. The fibrous membranes produced by electrospinning have high porosity, fine fiber diameters, large surface area-to-volume ratio, good interconnected pore structures and great permeability.[17,18]

To fabricate a dialysis membrane, zeolites were incorporated into electrospun PAN (polyacrylonitrile) polymeric nanofiber membranes. PAN porous membranes have a variety of excellent characteristics including good thermal and mechanical stability, tolerance to bacteria, and photo irradiation,[19] and excellent membrane forming properties.[20] PAN membrane made through traditional phase inversion method are used as a dialyzer membrane in clinic.[21–23]

In this paper we fabricated and characterised PAN nanofiber membranes and PAN-zeolite composite membranes with two types of zeolite, 840-NHA and 940-HOA, at differing concentrations (5, 10, 15, 20, 25, 30, and 35 wt %). Then, the creatinine absorption capacity of both free zeolites and incorporated zeolites were evaluated. We anticipate that PAN-zeolite membrane will have a quick speed to eliminate uremic toxins because of the fast adsorption speed of zeolites. The fibrous PAN-zeolite membrane which combine adsorption and diffusion together, could be a new choice for dialysis membranes.

## EXPERIMENTAL

### Materials

Polyacrylonitrile (PAN) with molecular weight of 150,000, dimethylformamide (DMF) and creatinine were purchased from Sigma Aldrich, Co. HSZ-series zeolites 500-KOA (L), 720-KOA (Farrierite), 840-NHA (ZSM-5), and 940-HOA (Beta) powders were purchased from Tosoh. Ultrapure water was also used.

### Preparation of Nanofibrous PAN Membranes

PAN electrospun solutions were prepared by dissolving 6, 8, and 10 wt % PAN powders in DMF at 60°C for 12 h. The PAN nanofibrous membranes were prepared using a laboratory set-up electrospinning equipment. The electrospun voltage was 22.5 kV, feed rate was 1 mL $h^{-1}$ and tip to collector distance was 15 cm. The relative humidity and temperature were kept between 48−52% and 23−26°C respectively. In all experiments, 21-gauge needles were used.

### Preparation of PAN-Zeolite Composite Membranes

PAN-zeolites solutions were prepared by adding zeolite powders into 10 wt % PAN electrospun solution from section 2.2. The composite solution was further stirred at room temperature for 12 h and ultrasonicated for 1 h during the stirring process. Composite solutions with zeolite to PAN polymer ratio varied from 10 : 100, 15 : 100, 20 : 100, 25 : 100, 30 : 100 to 35 : 100 were prepared. If a sample contains 10 wt % 840-NHA in PAN polymer, the samples were named 10−840, other samples were also named accordingly. The electrospinning factors were kept the same as section 2.2 except for the tip to collector distance, which was 19 cm. At this distance, a flat composite membranes were obtained smoothly.

### Scanning Electron Microscopy (SEM)

The morphology of PAN and PAN-zeolite membranes was examined using a Zeiss scanning electron microscope. The diameter of the fibers was measured by ImageJ software for 50 times. The PAN membranes and PAN-zeolite membranes were also examined by energy dispersive X-ray spectroscopy (EDX) equipped in SEM.

### Thermal Gravimetric Analysis (TGA)

Thermal gravimetric analysis (TGA) of the samples was conducted using the Q500 TGA instrument from TA Instruments. The temperature scans were taken from room temperature to 800°C at 10°C $min^{-1}$ in an ambient atmosphere at an air flow of 20 mL $min^{-1}$.

### Adsorption Studies of Zeolite Powders

UV-Visible spectrophotometer (Ultraspec 2100 pro) was used to measure the absorbance of the creatinine solution. Creatinine solutions with various concentrations (50, 100, 150, 200, 250, 312.5, and 400 μmol $L^{-1}$) were made by adding creatinine powders into beakers with ultrapure water and then stirred overnight.

An UV calibration standard line for creatinine in ultrapure water was prepared based on the absorption value of creatinine solutions at 234 nm. Creatinine solutions with concentration of 50 μmol $L^{-1}$, 100 μmol $L^{-1}$, 150 μmol $L^{-1}$, 200 μmol $L^{-1}$, and 250 μmol $L^{-1}$ were tested for drawing the UV calibration standard line.

Creatinine adsorption capacity of free zeolite was first tested by the following procedure. 0.025 g 500 KOA, 720 KOA, 840-NHA and 940-HOA powders were added into 4 vials with 10 mL 200 μmol $L^{-1}$ creatinine solution and were shaken at 37°C for 3 h at a speed of 165 rpm in a shaker (C25, New Brunswick Scientific, USA). The adsorption speed of 940-HOA powders was further measured using the same procedure by shaking them for 5, 10, 15, 20, and 25 min. Finally, the adsorption capacity of 940-HOA powders in 50 μmol $L^{-1}$, 200 μmol $L^{-1}$, 312.5 μmol $L^{-1}$, and 625 μmol $L^{-1}$ creatinine solutions were also measured for both 10 and 20 min.

### Adsorption Study of Zeolites Incorporated in Membranes

Creatinine adsorption capacities of different composite membranes were tested in a flow state according to the following procedure. First, composite membranes with a diameter of 10 mm were cut and positioned in a syringe filter cartridge (EMD Millipore, CA). Then, 200 μmol $L^{-1}$ creatinine solution was introduced into the inlet of the cartridge to flow through the membrane and exit through the outlet at the flow rate of 1 mL $h^{-1}$ for 3 h. Finally, UV absorption spectrums of solutions collected from the outlet were measured. Four samples of each type of membrane were tested. The creatinine adsorption capacity of 30−940 membranes with different thicknesses were further measured following the same procedure.

## RESULTS AND DISCUSSION

### Fabrication of PAN Membranes

Electrospinning is a process based on electrohydrodynamics to form continuous thin fibers, which can further form fibrous

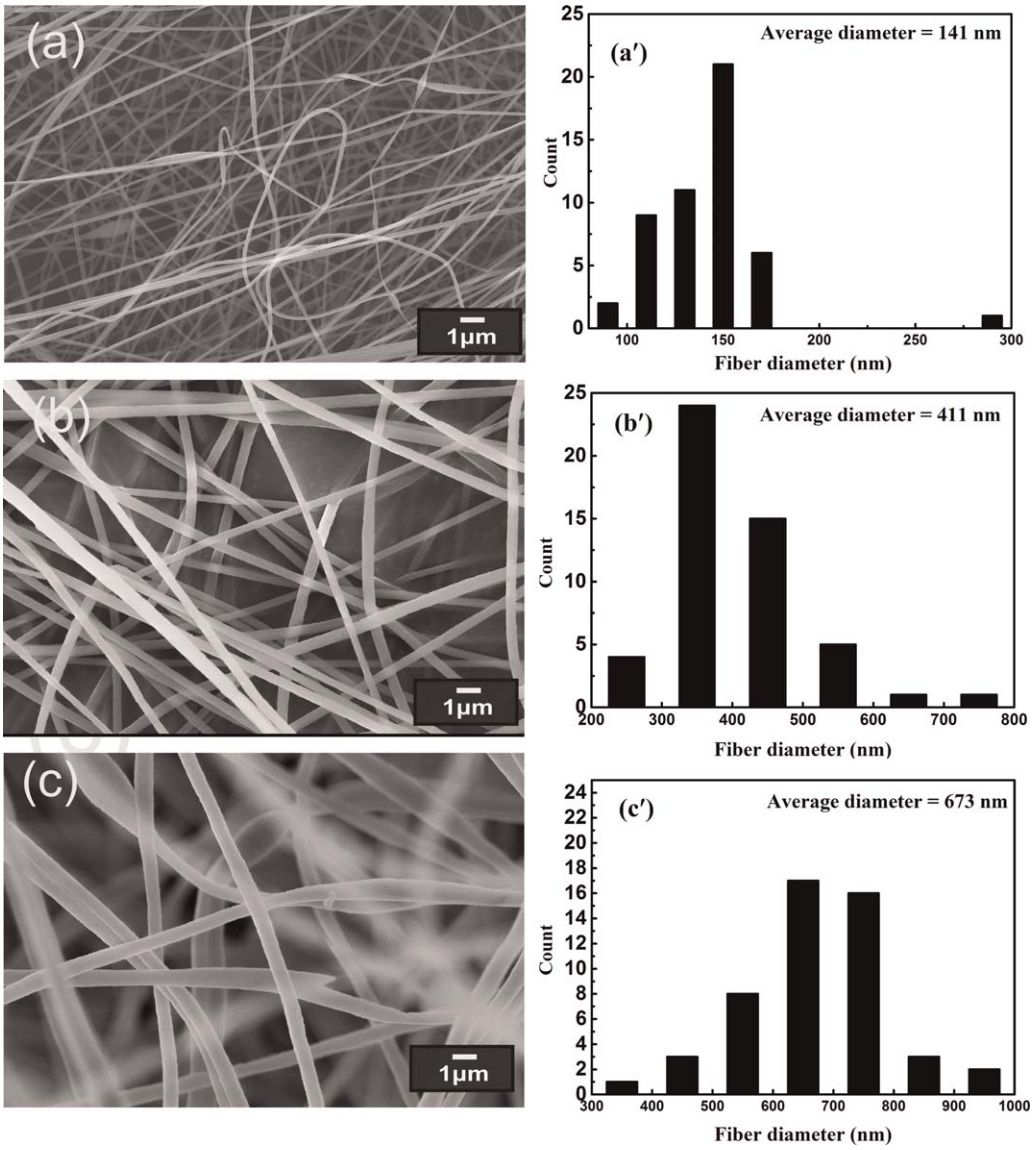


**Figure 1.** SEM images and diameters of electrospun PAN nanofibers produced in DMF with polymer concentrations of 6 wt % (a), 8 wt % (b), and 10 wt % (c).

membranes.[24] This membrane fabrication method is simple, easy, and cost-effective. Various polymers have been used in electrospinning processes.[25–28] Among them, electrospun PAN membranes have attracted much attention due to its excellent thermal stability and insolubility to most solvents.[29] PAN-based membranes have been widely used in water treatment,[30,31] protein filtration and dialysis.[22] In this paper, PAN fibrous membranes with different concentrations were fabricated by adjusting voltage, tip to collector distance, flow rate, temperature, and humidity during the electrospinning process. The best conditions to get smooth fibers were at 22.5 kV with a flow rate of 1 mL $h^{-1}$ in a relative humidity of 50% at 25°C. These conditions were used in the following experiments. The morphology of the fibers with 6, 8, and 10 wt % of PAN in DMF is shown in Figure 1. Smooth fibers with rare beads are observed in all the figures. The rare beads in Figure 1 have probably formed due to the disturbance of electrospinning parameters, such as flow rate, humidity, voltage and current. The diameter of fibers with 6 wt % of PAN is 141 nm, which is the thinnest among all the three samples. The diameter of 8 wt % of PAN is 411 nm and that of 10 wt % of PAN is 673 nm. Typically, the fiber diameter would increase with increased polymer concentration when other fabrication factors are unchanged. Solutions with more than 15 wt % of PAN in DMF were not used since their viscosities were too high for the electrospinning apparatus.

### Fabrication of PAN-Zeolite Membranes

Polymeric membranes filled with zeolites have their advantages since they combine molecular sieve property of zeolites and processability of polymers.[12] Polymer−zeolite membranes have been used for gas separation,[12,32] ethanol−water separation,[33] and water treatment.[34] To maintain a relatively high flow rate of 1 mL $h^{-1}$, the 10 wt % PAN in DMF was chosen as the polymer solution base for incorporating zeolites. To better distribute the

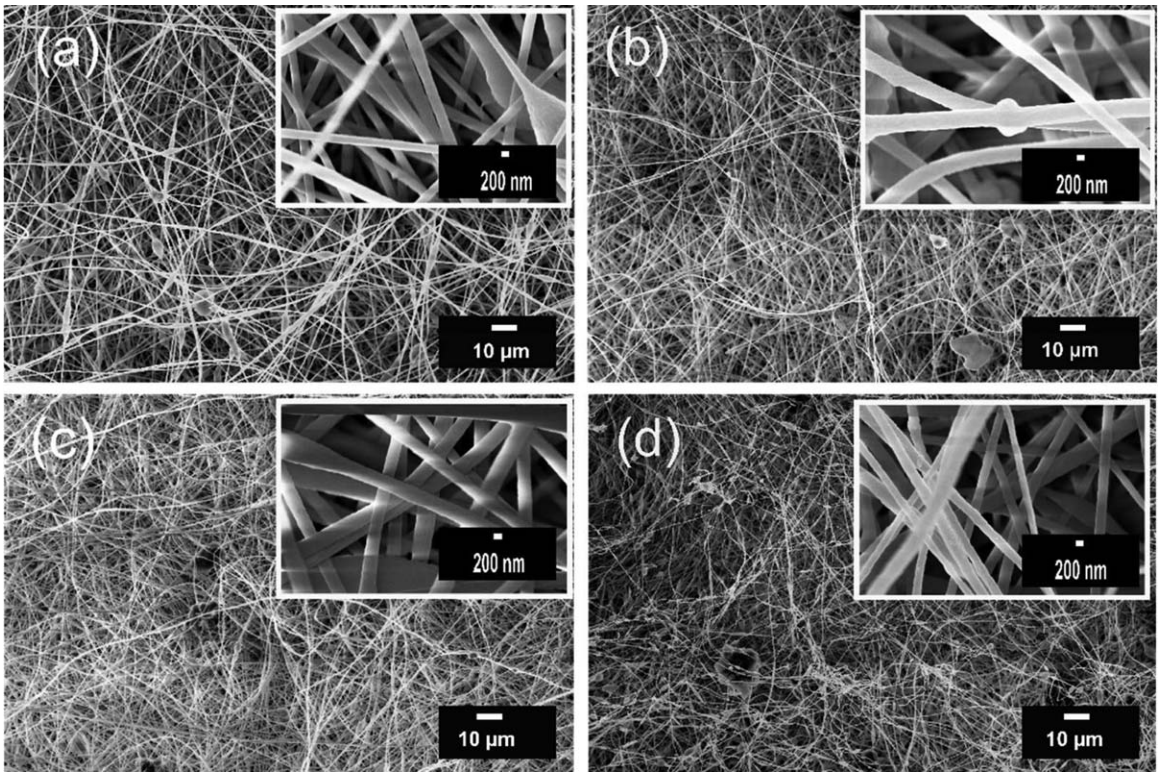


**Figure 2.** SEM images of PAN-zeolite nanofibrous composite membranes. 10−940 (a), 30−940 (b), 25−840 (c), and 30−840 (d). (PAN is 10 wt % based).

zeolites within the polymer, the composite solution was stirred for over 12 h before electrospinning. Furthermore, the solutions were ultrasonicated twice for 30 min during the stirring process.

Figure 2 shows SEM images of PAN-zeolite composite membranes with 940 (10 and 30 wt %) and 840 (25 and 30 wt %). In these images, a mix of bead and fiber morphology can be observed. The formation of beads was due to relatively large zeolite particle sizes (0.67−2 μm) when compared with fiber diameters (277−419 nm, shown in Supporting Information Fig. S1). Another potential reason was due to poor distribution or aggregation of zeolite particles. However, smooth nanofibers existed between the beads. Supporting Information Figure S1 shows a comparison between the average fiber diameter of PAN and PAN-zeolite membranes. The fiber diameter of 10 wt % PAN membrane without zeolites was 675 nm while the fiber diameter in the membrane with 10 wt % 940 [Figure 2(a)] was 277 nm and that in the membrane with 30 wt % 940 [Figure 2(b)] was 398 nm. It further indicated that the fiber diameter in the membrane with 25 wt % 840 [Figure 2(c)] was 419 nm while that in the membrane with 30 wt % 840 [Figure 2(d)] was 277 nm. From these data we know that the membrane with zeolites had decreased fiber diameter when compared with PAN membrane and the fiber diameters in PAN-zeolite membrane were relevant to zeolite type (size and shape) and concentrations. The properties of zeolites used in this paper are provided in Supporting Information Table S1.

To further determine the successful incorporation of zeolites into the membrane, SEM/EDX Si-mapping images are presented in Figure 3. Silicon atom was chosen for it existed in zeolites, but not in PAN polymers. EDX analysis further presented the Silicon atomic percentages in PAN and PAN-zeolite membranes, show in Supporting Information Table S2. There are merely 0.07% Silicon atoms in PAN membranes while 14.01% in the membrane with 10 wt % 940. Figure 3(a,b) is the Si-mapping of 10 wt % 940-HOA PAN membranes; no aggregation of Si was observed. Contrarily, large areas of Si aggregation were observed in membranes with 30 wt % 940-HOA [Fig. 3(c,d)]. Uniform distributions of zeolite within the membrane were harder to achieve when incorporating higher concentration zeolite. Similarly, mildly aggregation were observed in Figure 3(e,f), which had 25 wt % of 840-NHA.

TGA testing was further carried out to precisely determine the percentage of zeolites inside the membranes. At 800°C, PAN polymer is totally burned and only zeolites are left on the pan. As indicated in Figure 4, PAN membrane [Figure 4(a)] had 0 weight left at 800°C. 10–10940 [Figure 4(b)] had 10% weight left at 800°C. This indicated that 100% of the fed zeolites are incorporated inside the membranes. Similarly, 10–20940 [Figure 4(c)] had 18% weight left at 800°C, which indicated that 90% of the fed zeolites (20 wt % 940) were incorporated into the membranes. The membranes fed with 30 wt % zeolite had around 24 wt % of zeolites inside the membrane [as shown in 10–30 940, Figure 4(d)]. From the TGA analysis we can see that the deviation between the zeolite in feed and zeolites in membrane grew larger with increased zeolite feeding percentages. The date from Supporting Information Table S3 further supported this.

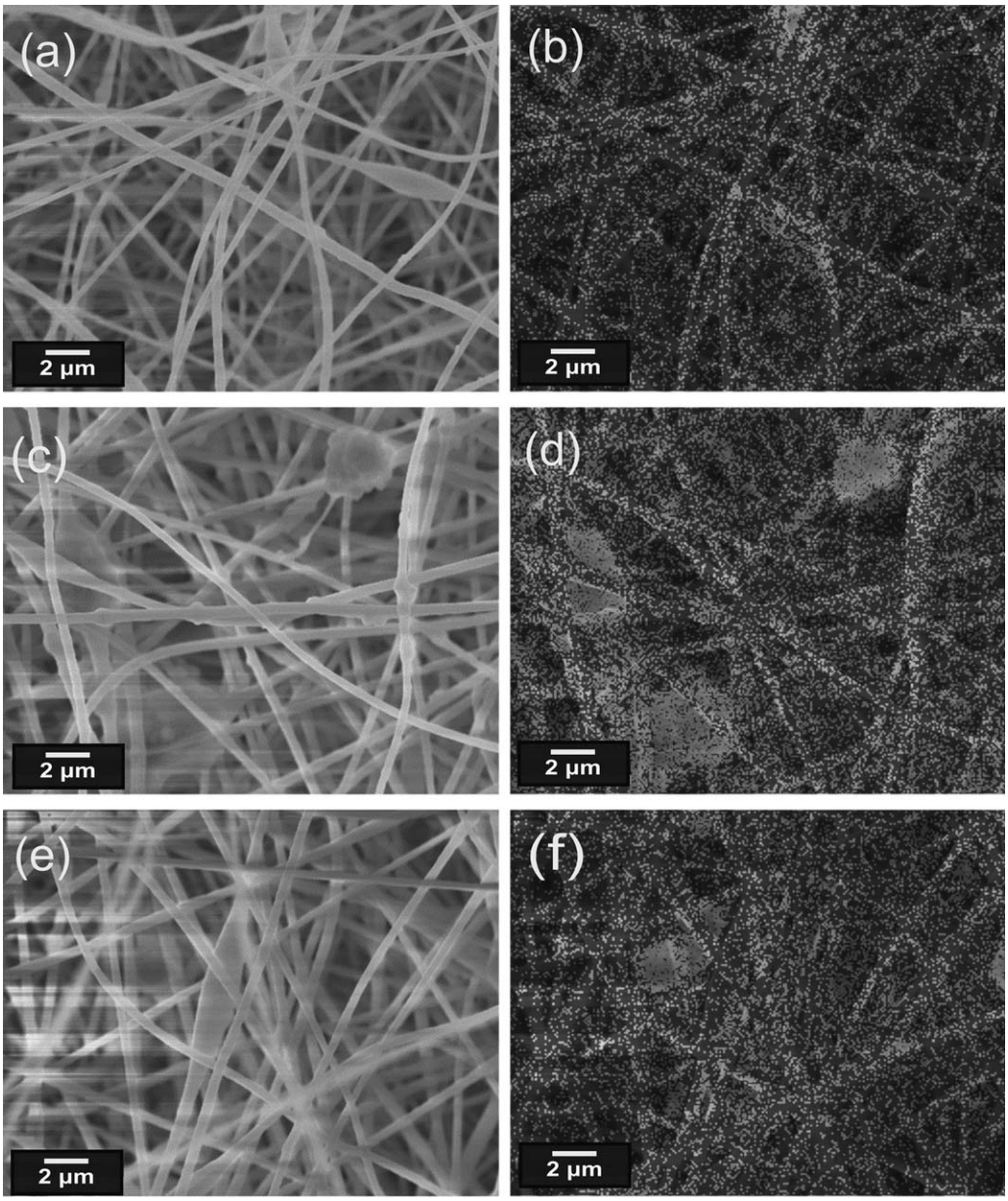


**Figure 3.** SEM/EDX mapping images of zeolite-PAN membrane with zeolites: 10−940 (a) with Si-mapping (b), 30−940 (c) with Si-mapping (d), and 25−840 (e) with Si-mapping (f).

The above analysis shows that zeolite-PAN nanofiber membranes can be successfully fabricated through the electrospinning method. However, with increased zeolite fed percentage, it is harder to incorporate all the zeolites in the membrane and higher percentage of zeolites tend to coagulate inside the membranes.

### Creatinine Adsorption Capacity of Zeolites

To determine the creatinine adsorption capacity of zeolite, several experiments were designed and carried out. Figure 5(a) presents the adsorption capacity of various zeolite in both 200 μmol $L^{-1}$ and 50 μmol $L^{-1}$ creatinine solutions for a 3 h period. 500-KOA were nonadsorbent to creatinine since their pore size was smaller than that of creatinine.[35] 720-KOA and 840-NHA reduced 10% and 42% of creatinine in 200 μmol $L^{-1}$ creatinine solution, and a relatively higher percentage (27% and 58%) in 50 μmol $L^{-1}$ creatinine solution. 940-HOA had the best creatinine adsorption capacity; almost all the creatinine from both 200 μmol $L^{-1}$ and 50 μmol $L^{-1}$ creatinine solution was adsorbed. Figure 5(b) exhibits the creatinine adsorption capacity of zeolites by zeolite mass. 940-HOA's creatinine adsorption capacity is as high as 9050 μg $g^{-1}$ in a 200 μmol $L^{-1}$ solution, which was four times of that in 50 μmol $L^{-1}$ creatinine solution. This experiment revealed that creatinine adsorption capacity was related to the initial concentration of creatinine solution as well as zeolite type.

940-HOA was chosen to further evaluate its creatinine adsorption speed. Supporting Information Figure S1 demonstrates that the adsorption speed of zeolites was very quick, 0.025 g of 940-HOA

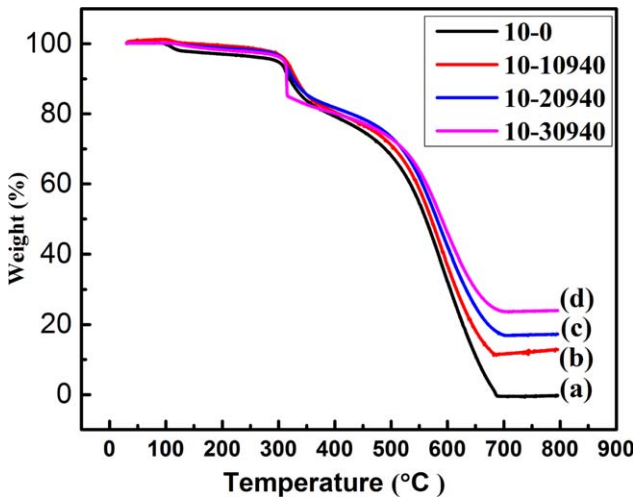


**Figure 4.** TGA analysis of composite membranes. [Color figure can be viewed in the online issue, which is available at wileyonlinelibrary.com.]

powders adsorbed 91% of creatinine from 10 mL 200 μmol $L^{-1}$ creatinine solution in 5 min and 96% of that in 10 min.

To further reveal how initial creatinine solution and adsorption time affected creatinine adsorption capacity of zeoiltes, 940-HOA powders were added to creatinine solutions with concentrations from 50 to 625 μmol $L^{-1}$ for both 10 min and 20 min. Figure 6(a) showed that, in 10 min, 940 could adsorb 96, 96, 90, 76, and 70% of creatinine from 10 mL 50, 200, 312.5, 400, and 625 μmol $L^{-1}$ creatinine solution correspondingly. To express the data in adsorption capacity method, 940-HOA zeolite exhibited higher adsorption capacity with increased creatinine concentration, as shown in Figure 6(b). It had the lowest capacity (5430 μg $g^{-1}$) in 50 μmol $L^{-1}$ creatinine solution, a gradually increased capacity in (8639, 13621, and 14126 μg $g^{-1}$) 200, 312.5, and 400 μmol $L^{-1}$ creatinine solution, and the greatest capacity (25,452 μg $g^{-1}$) in 625 μmol $L^{-1}$ creatinine solution. The adsorption capacity of 940-HOA varied little within 10 min and 20 min. This further exhibited that the adsorption speed of creatinine was very quick.

### Creatinine Adsorption Capacity of Zeolite-PAN Membranes in a Flow State

All the membranes used in this experiment were electrospun for 1 h at a flow rate of 1 mL $h^{-1}$. To test the creatinine adsorption capacity of PAN-zeolite membranes, the membranes were cut into 10 mm disks and then mounted in syringe filter cartridges. A solution of 200 μmol $L^{-1}$ creatinine was filtered through the membrane at a rate of 1 mL $h^{-1}$ for 3 h. Figure 7(a) reveals that the membranes with 840-NHA or 940-HOA zeolites could successfully adsorb creatinine at distinct levels. Among the membranes with 840-NHA, the membrane with 25 wt % zeolites (10−25) reduced as much as 43% creatinine in 3 h. Similarly, within all the membranes with 940-HOA, 10−30 reduced 52% of the creatinine in solution. Figure 7(b) presents the creatinine adsorption capacity of each membrane by membrane mass as well as zeolite mass. Similarly, 10−25 membranes with 840-NHA and 10−30 membranes with 940-HOA both showed the highest creatinine adsorption capacity by membrane mass: 2545 μg $g^{-1}$ and 2658 μg $g^{-1}$ respectively. Figure 7(b) demonstrates that the membrane with 10 wt % zeolite had the highest creatinine adsorption value by zeolite mass (19,117 μg $g^{-1}$for 840-NHA and 14140 μg $g^{-1}$ for 940-HOA). A potential reason was that the zeolite distribution was more uniform and less aggregated inside the membrane at low zeolite level, as supported by Figure 3.

By collecting the membranes over different spinning times while keeping all the other experimental factors the same, we could get membranes with various thicknesses. Supporting Information Figure S2 shows the creatinine adsorption capacity of membranes with various thicknesses. It shows that, the thinner the membrane, the higher the creatinine adsorption capacity by membrane mass and zeolite mass. The membranes collected for 0.5 h at a flow rate of 1 mL $h^{-1}$ is recommended, since it had good creatinine absorption capacity as well as the potential for high mechanical strength.

Creatinine concentration for a healthy person is normally less than 106 μmol, while that of patients with kidney disease is around 1204 ± 407 μmol. The creatinine adsorption capacity of

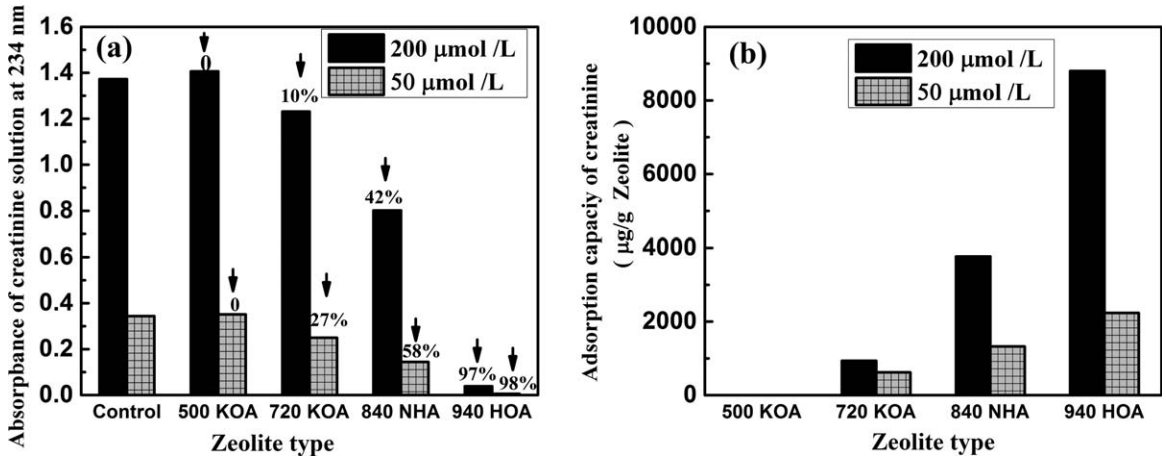


**Figure 5.** Creatinine adsorption capacity of zeolites in 200 μmol $L^{-1}$ and 50 μmol $L^{-1}$ creatinine solution for 3 h. The absorbance values of creatinine solution and the adsorption percentage (a); Creatinine adsorption capacity of zeolites by zeolite mass (b).

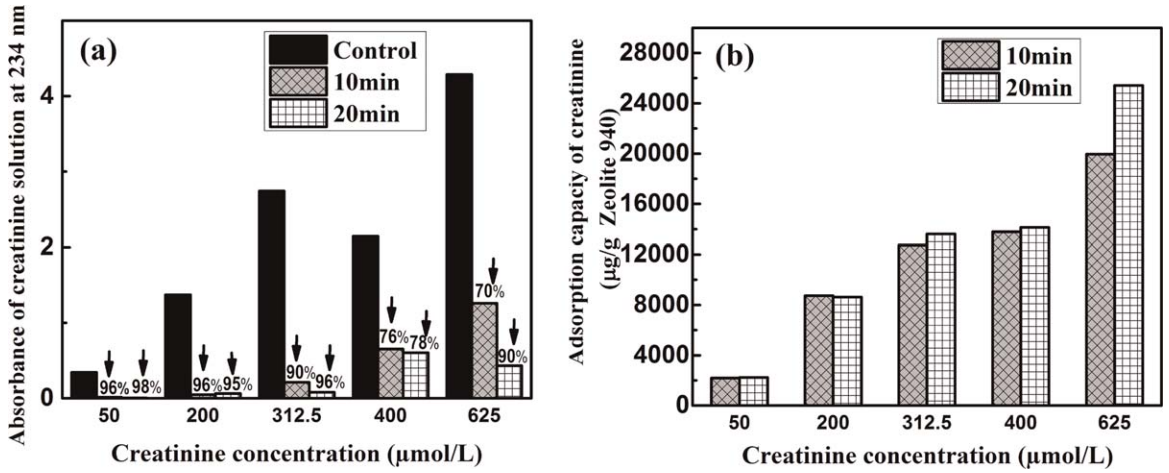


**Figure 6.** Creatinine adsorption capacity of 940-HOA zeolites in different creatinine concentration and for both 10 min and 20 min. The absorbance value of creatinine solution and the adsorption percentage (a); Creatinine adsorption capacity of zeolite by zeolite mass (b).

940-HOA increased from 2262 μg $g^{-1}$ in 50 μmol $L^{-1}$ creatinine solution to 25,423 μg $g^{-1}$ in 625 μmol $L^{-1}$ creatinine solution. We can expect better creatinine adsorption capacity of 940-HOA in solutions with higher creatinine concentration. Furthermore, the adsorption speed of 940-HOA is very quick (0.025 g 940-HOA will eliminate 91% of 20 μmol creatinine in 5 min).

When we compared the creatinine adsorption capacity of zeolite powder and that of zeolite incorporated in membranes, zeolite showed improved capacity inside the membrane. Specifically, the creatinine adsorption capacity was 3733 μg $g^{-1}$ for 840 powders while it was 19,230 μg $g^{-1}$ for 840 inside the membrane. On the other hand, the capacity of 940-HOA powders was 8823 μg $g^{-1}$ while it was 13,574 μg $g^{-1}$ for 940 inside the membrane. The fact that 840 and 940 zeolites had improved capacity inside the membranes might be because of the following two reasons. First, the zeolites particles tended to coagulate even though they were shaken at 165 rpm during test since there is no force to separate zeolites particles. However, they were better distributed in the polymer matrix after stirring overnight. As a result, the effective surface area of zeolites to adsorb creatinine was largely increased in the membranes. The second reason is related to the testing method. The adsorption capacity of zeolite powder was tested inside vials by shaking them at 165 rpm. And the composite membrane was tested in flow state.

We also noticed that the creatinine adsorption capacity of 840 in membrane improved four times compared with that of 840 powders while that of 940-HOA improved merely 0.5 times in the membrane when comparing with 940 powder. This is possibly because the mean particle size of 840-NHA was 2 μm while that of 940-HOA was 0.67 μm. 840-NHA powders had significantly larger particle diameters when compared with the PAN fiber diameters (277−410 nm), so a lower percentage of zeolite particle surface was blocked by fibers. On the other hand, 940 had closer particle size to the PAN fiber diameters (276−398 nm), thus 940 zeolite powders can be buried inside the zeolites easily.

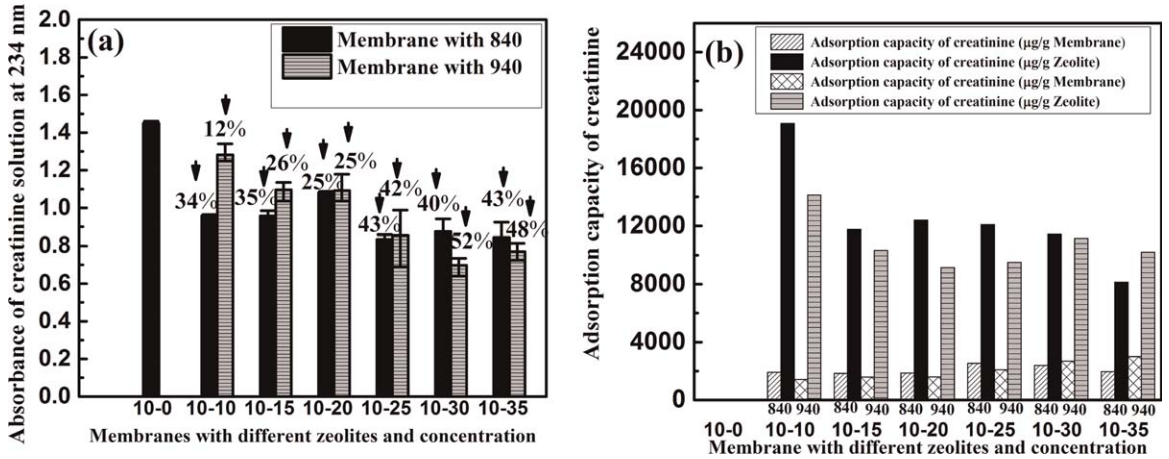


**Figure 7.** Creatinine adsorption capacity of membranes with different concentration of 840-NHA and 940-HOA under flow state in 200 μmol $L^{-1}$ creatinine solution for 3 h. The absorbance value of creatinine solution and the creatinine adsorption percentage was shown in (a); creatinine adsorption capacity of zeolites by fiber mass and zeolite mass were presented in (b).

Future work will investigate how the particle size of zeolite affects the adsorption capacity of PAN-zeolite membranes as well as explore the possibility of using PAN-zeolite to eliminate creatinine from blood.

## CONCLUSIONS

In summary, this study successfully fabricated PAN-zeolite nanofibrous membranes through an electrospinning process. Creatinine adsorption capacity of the zeolite as free powder was compared with the zeolite incorporated into membranes. The membrane with 10 wt % zeolite had the highest creatinine adsorption capacity by zeolite mass; for at low zeolite ratio they could be uniformly incorporated inside the membrane. It was also shown that creatinine adsorption of zeolite was strongly affected by creatinine concentration. The membranes collected for 0.5 h at flow rate of 1 mL $h^{-1}$ are recommended when considering adsorption efficiency and processability. By comparing the creatinine adsorption capacity of 840-NHA and 940-HOA, the particle size and the surface area play an important role in determining the functional effects of the membranes.

## ACKNOWLEDGMENTS

This work was supported by the Natural Sciences and Engineering Research Council of Canada (NSERC) and University of Waterloo.

## REFERENCES

1. Collins, A. J.; Foley, R. N.; Chavers, B.; Gilbertson, D.; Herzog, C.; Ishani, A.; Johansen, K.; Kasiske, B. L.; Kutner, N.; Liu, J. *Am. J. Kidney Dis.* **2014**, *63*, A7.
2. Oodan, T.; Hasegawa, I.; Ooishi, R.; Nishiyama, T.; Amemiya, H.; Okuyama, H.; Kobayashi, T.; Akizawa, T.; Ideura, T.; Hiyoshi, T.; Miyazaki, T. *Jpn. J. Artif. Organs* **1997**, *26*, 418.
3. Kandus, A.; Malovrh, M.; Bren, A. F. *Artif. Organs* **1997**, *21*, 903.
4. Hoenich, N. A.; Stamp, S.; Roberts, S. J. *ASAIO J.* **2000**, *46*, 70.
5. Namekawa, K.; Kaneko, A.; Sakai, K.; Kunikata, S.; Matsuda, M. *J. Artif. Organs* **2011**, *14*, 52.
6. Vanholder, R.; Argilés, A.; Baurmeister, U.; Brunet, P.; Clark, W. *Int. J. Artif. Organs* **2001**, *24*, 695.
7. Wernert, V.; Schäf, O.; Ghobarkar, H.; Denoyel, R. *Microporous Mesoporous Mater.* **2005**, *83*, 101.
8. Bergé-Lefranc, D.; Pizzala, H.; Paillaud, J. L.; Schäf, O.; Vagner, C.; Boulet, P.; Kuchta, B.; Denoyel, R. *Adsorption* **2008**, *14*, 377.
9. Bergé-Lefranc, D.; Eyraud, M.; Schäf, O. *Comptes Rendus Chimie* **2008**, *11*, 1063.
10. Bergé-Lefranc, D.; Vagner, C.; Schäf, O.; Boulet, P.; Pizzala, H.; Paillaud, J.; Denoyel, R. *Stu. Surf. Sci. Catal.* **2007**, *170*, 1015.
11. Bergé-Lefranc, D.; Pizzala, H.; Denoyel, R.; Hornebecq, V.; Bergé-Lefranc, J. L.; Guieu, R.; Brunet, P.; Ghobarkar, H.; Schäf, O. *Microporous Mesoporous Mater.* **2009**, *119*, 186.
12. Pechar, T. W.; Kim, S.; Vaughan, B.; Marand, E.; Tsapatsis, M.; Jeong, H. K.; Cornelius, C. J. *J. Membr. Sci.* **2006**, *277*, 195.
13. Moreno, N.; Querol, X.; Ayora, C.; Pereira, C. F.; Janssen-Jurkovicová, M. *Environ. Sci. Technol.* **2001**, *35*, 3526.
14. Álvarez-Ayuso, E.; García-Sánchez, A.; Querol, X. *Water Res.* **2003**, *37*, 4855.
15. Cheng, Z.; Chao, Z.; Wan, H. *Prog. Chem.* **2004**, *16*, 61.
16. Chaidou, C. I.; Pantoleontos, G.; Koutsonikolas, D. E.; Kaldis, S. P.; Sakellaropoulos, G. P. *Separation Sci. Technol. (Philadelphia)* **2012**, *47*, 950.
17. Ma, H.; Hsiao, B. S.; Chu, B. *J. Membr. Sci.* **2014**, *452*, 446.
18. Chen, J. C.; Wu, J. A.; Lin, K. H.; Lin, P. J.; Chen, J. H. *Polym. Eng. Sci.* **2014**, *54*, 430.
19. Wang, Z. G.; Wan, L. S.; Xu, Z. K. *J. Membr. Sci.* **2007**, *304*, 8.
20. Chen, X.; Su, Y.; Shen, F.; Wan, Y. *J. Membr. Sci.* **2011**, *384*, 44.
21. Pascual, M.; Schifferli, J. A. *Kidney Int.* **1993**, *43*, 903.
22. Lin, W.-C.; Liu, T.-Y.; Yang, M.-C. *Biomaterials* **2004**, *25*, 1947.
23. Smeby, L. C.; Widerøe, T.-E.; Balstad, T.; Jørstad, S. *Blood Purif.* **1986**, *4*, 93.
24. Obaid, M.; Fadali, O. A.; Lim, B.-H.; Fouad, H.; Barakat, N. A. M. *Mater. Lett.* **2015**, *138*, 196.
25. Ma, Z.; Kotaki, M.; Ramakrishna, S. *J. Membr. Sci.* **2005**, *265*, 115.
26. Bae, H. S.; Haider, A.; Selim, K. M. K.; Kang, D. Y.; Kim, E. J.; Kang, I. K. *J. Polym. Res. 20*, **2013**.
27. Nirmala, R.; Navamathavan, R.; Park, S. J.; Kim, H. Y. *Nano-Micro Lett.* **2014**, *6*, 89.
28. Krupa, A.; Jaworek, A.; Sundarrajan, S.; Pliszka, D.; Ramakrishna, S. *Fibres Text. Eastern Europe* **2012**, *91*, 25.
29. Zhang, G.; Meng, H.; Ji, S. *Desalination* **2009**, *242*, 313.
30. Cao, X.; Huang, M.; Ding, B.; Yu, J.; Sun, G. *Desalination* **2013**, *316*, 120.
31. Yoon, K.; Hsiao, B. S.; Chu, B. *J. Membr. Sci.* **2009**, *338*, 145.
32. Ahn, J.; Chung, W. J.; Pinnau, I.; Guiver, M. D. *J. Membr. Sci.* **2008**, *314*, 123.
33. Vane, L. M.; Namboodiri, V. V.; Bowen, T. C. *J. Membr. Sci.* **2008**, *308*, 230.
34. Zadaka-Amir, D.; Nasser, A.; Nir, S.; Mishael, Y. G. *Microporous Mesoporous Mater.* **2012**, *151*, 216.
35. Namekawa, K.; Tokoro Schreiber, M.; Aoyagi, T.; Ebara, M. *Biomater. Sci.* **2014**, *2*, 674.